Frequency Ratio Approach for Landslide Susceptibility Mapping of Phonda Ghat of Maharashtra

Chapter · April 2022

DOI: 10.1007/978-981-16-7731-1_2

3 authors:

Abhijit S. Patil
Shivaji University, Kolhapur
15 PUBLICATIONS **52** CITATIONS
SEE PROFILE

Sachin Shantaram Panhalkar
Shivaji University, Kolhapur
39 PUBLICATIONS **274** CITATIONS
SEE PROFILE

Sambhaji Dnyaneshwar Shinde
Shivaji University, Kolhapur
67 PUBLICATIONS **131** CITATIONS
SEE PROFILE

Advances in Geographical and Environmental Sciences

R. B. Singh
Manish Kumar
Dinesh Kumar Tripathi *Editors*

Remote Sensing and Geographic Information Systems for Policy Decision Support

Springer

Chapter 2
Frequency Ratio Approach for Landslide Susceptibility Mapping of Phonda Ghat of Maharashtra

Abhijit S. Patil, S. S. Panhalkar, and Sambhaji D. Shinde

Abstract The Western Ghats of Maharashtra frequently suffer from landslides caused by various geo-environmental factors. The prime aim of this study is to produce a suitable landslide susceptibility map of the Phonda Ghat region of Western Ghats of Maharashtra. The present study reveals the application of the Frequency Ratio (FR) model using GIS techniques to assess the influence of geo-environmental factors on the occurrence and distribution of landslides. The FR model is derived from the landslide inventory and geo-environmental factors viz, Slope angle, Slope curvature, Aspect, Relief, Drainage, Land Use/Land Cover, Lineament, Geology, NDVI, Geomorphology, Rainfall, and Soil depth. The main focus of this investigation is to categorize the land surface of the study area on the basis of the degree of potential landslide susceptibility. The model is validated by performing the AUC curve method. The result shows the landslide susceptibility map, which demarcated more than 13% of the land area of the study region, is highly potential to the landslide.

Keywords Frequency ration (FR) · Phonda ghat · GIS · Landslide susceptibility

2.1 Introduction

Landslides are natural hazards that are caused by several geophysical & anthropogenic factors. These landslides are dangerous, occur suddenly, and cause significant damages (Guzzetti et al. 1999). Generally, landslides occur in mountainous and rugged terrain all over the world. The Himalayas and Western Ghats of India characterize highly undulating and mountainous terrain. The Western Ghats contain a significant highland range running parallel to the western coast of India. Several studies on landslide mapping have shown that the Western Ghats region of India is highly vulnerable to landslide hazards (Ramchandra et al. 2010; Patil et al. 2019). Remote Sensing (RS) and Geographical Information Systems (GIS) play a crucial role as they are used as the leading tools for detection, classification, analysis, and

A. S. Patil · S. S. Panhalkar (✉) · S. D. Shinde
Department of Geography, Shivaji University Kolhapur, Kolhapur, Maharashtra, India

R. B. Singh et al. (eds.), *Remote Sensing and Geographic Information Systems for Policy Decision Support*, Advances in Geographical and Environmental Sciences,
https://doi.org/10.1007/978-981-16-7731-1_2

mapping of landslides. Recently, landslide hazard mapping is quite possible due to easy access and a fine resolution of remote sensing data and thematic layers using Geographical Information Systems (Gupta et al. 1990; Scaioni 2013; Qiao et al. 2013). The study of landslide hazard mapping based on Remote Sensing and GIS techniques is carried out by a number of authors (Mantovani et al. 1996; Gupta et al. 1999; Saha et al. 2002; Lee et al. 2007). In recent times, a number of methods and techniques of GIS and RS for landslide mapping have been proposed and applied (Wang et al. 2005; Pardeshi et al. 2013; Balasubramani K et al. 2013; Merrett et al. 2013; Patil et al. 2020).

The advances in GIS and Multi-Criteria Decision Analysis (MCDA) have changed the perspective of the landslide study. The integration of GIS and MCDA creates new tools that help for the management of data and spatial analysis (Guzzetti et al. 1999; Kayastha et al. 2013). Bayes Ahmed (2014) has used three different methods of Geographical Information System based on Multi-Criteria Decision Analysis methods. Artificial Hierarchy Process (AHP), Weighted Linear Combination (WLC), and Ordered Weighted Average (OWA) were applied scientifically to assess the landslide susceptible areas in Chittagong Metropolitan Area, Bangladesh. van Wstern et al. (2011) have given an overview of a recent research project between GSI, the National Remote Sensing Centre (NRSC), and ITC (the Netherland) on how the existing technique for landslide inventory, susceptibility, and hazard assessment for India could be improved, and how these could be used for quantitative risk assessment. Westen et al. (1999) have made a comparative study of landslide hazard maps of the Alpago region in Italy to get a better insight into decision rules in their direct mapping approach and to improve GIS-based indirect mapping techniques. The present study has been carried out to demarcate the landslide susceptibility zone of the PhondaGhat region of Maharashtra using Remote Sensing and GIS techniques.

Over the last few years, landslide susceptibility assessment is considered as a significant and beneficial approach to predict the probability of spatial distribution of landslide occurrence under certain geo-environmental circumstances. Thus, it is valuable to do a landslide susceptibility assessment for landslide disaster risk reduction (Srivastava et al. 2010; Mahalingam et al. 2016; Persichillo et al. 2016).In the past years, many models have been applied for landslide susceptibility assessment, and these models can be mainly divided into qualitative models and quantitative models (Devkota et al. 2013; Wu et al. 2016). The frequency ratio (FR) is a quantitative model that can be easily applied and provides high accuracy for landslide susceptibility assessment (Lee and Talib 2005; Lee and Pradhan 2006; Yilmaz 2009).

2.2 Study Area

The entire study area is located towards the extreme southern part of the Maharashtra state of India. It lies between 16°17′35″N to 16°26′41″N latitude and 73°46′52″E to 73°56′ 37″E longitude thereby covering a total geographical area of approximately 291 km^2 (Fig. 2.1). It is extended in part of Kolhapur and Ratnagiri districts. The average height of the study area is about 525 m. The maximum height is 945 m, which is observed towards the ridgeline area of a western ghat in the study area. The lowest point is the extreme west part, where the height is 105 m above sea level. The parts of the Radhanagari reservoir, Kurli dam, Kalammawadi, and other small dams, have occupied 24.5 km^2 of the study region.

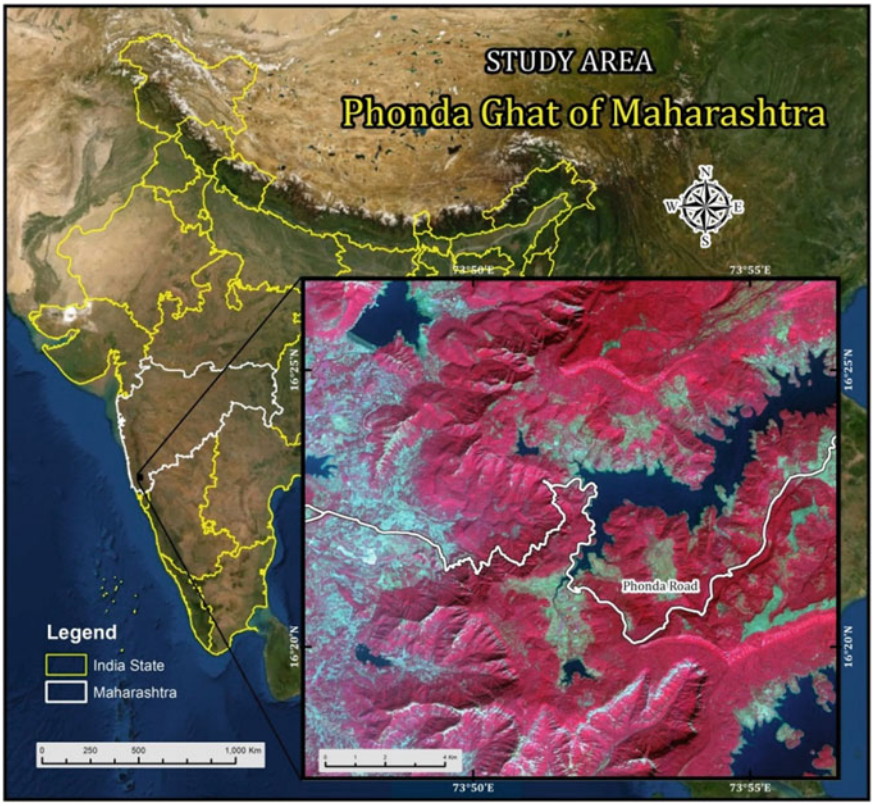

Fig. 2.1 Geographical location of study area

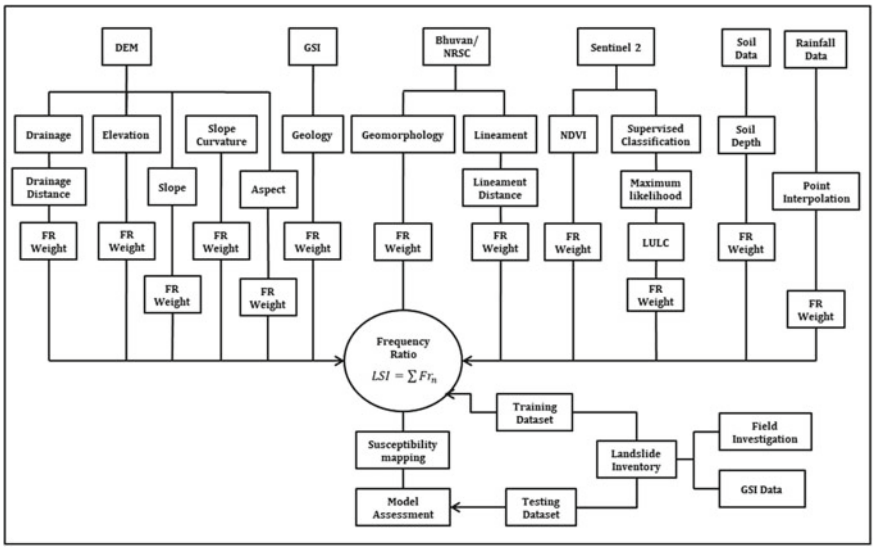

Fig. 2.2 Research methodology

2.3 Research Methodology

The processes of Landslide Susceptibility Assessment (LSA) include data sources preparation, landslide-related environmental factors analysis, and calculation of landslide susceptibility indexes (LSI). A precise and effective prediction of landslide susceptibility index is essential for producing the landslide susceptibility map (LSM).

The main object of this study is to prepare LSM using the Frequency Ratio model for the PhondaGhat region.

In the beginning, the landslide inventory and other data are obtained from different data sources and landslide-associated 12 geo-environmental factors are studied. Further, the FR values of these geo-environmental factors are calculated. Then third, the FR model is used to calculate the LSI based on landslide inventories, selected environmental factors, and field investigation data. Meanwhile, the LSM of the PhondaGhat area is produced in ArcGIS and QGIS software. Finally, to assess the reliability and efficiency of the method, the Area Under Curve (AUC) is calculated using a cumulative percentage of testing landslide inventory and susceptible zone. Figure 2.2 is providing a brief and systematic flow of entire research work.

2.3.1 *Frequency Ratio Method*

The FR method is used to study the relationships between past landslide sites and subclasses of each potentially influential factor (Lee and Min 2001; Lee and Pradhan 2006).In this investigation, all the influential factors are classified into their respective classes and the frequency ratio (Eq. 2.1.1) is calculated based on each class, i. Further, the normalized frequency ratio (Eq. 2.1.2) is computed for all classes in the same factor. The summation of the normalized frequency ratio of each influential factor results in the landslide susceptibility index (Eq. 2.1.3) (Pradhan and Lee 2010; Wang et al. 2016).

Fr_i (Frequency Ratio of class *i*):

$$\mathrm{Fr}_i = \frac{\left(\frac{\mathrm{NL}_i}{\mathrm{NL}_t}\right)}{\left(\frac{\mathrm{NC}_i}{\mathrm{NC}_t}\right)} \tag{2.1.1}$$

Fr_n (Normalized Frequency Ratio):

$$\mathrm{Fr}_n = \frac{\mathrm{Fr}_i}{\sum \mathrm{class}i\mathrm{Fr}\ ,} \tag{2.1.2}$$

LSI (Landslide Susceptibility Index):

$$\mathrm{LSI} = \sum \mathrm{Fr}_n \tag{2.1.3}$$

where

NL_i = number of landslides in class *i*.

NL_t = total number of landslide.

NC_i = number of cell points of class *i*.

NC_t = total number of cell points.

2.4 Result and Discussion

2.4.1 *Landslide Inventory*

The initial step to produce the landslide susceptibility map is the production of updated landslide inventory maps (Varnes 1984; Choi and Min 2004). The Geological Survey of India, field investigation, and local land resource departments have

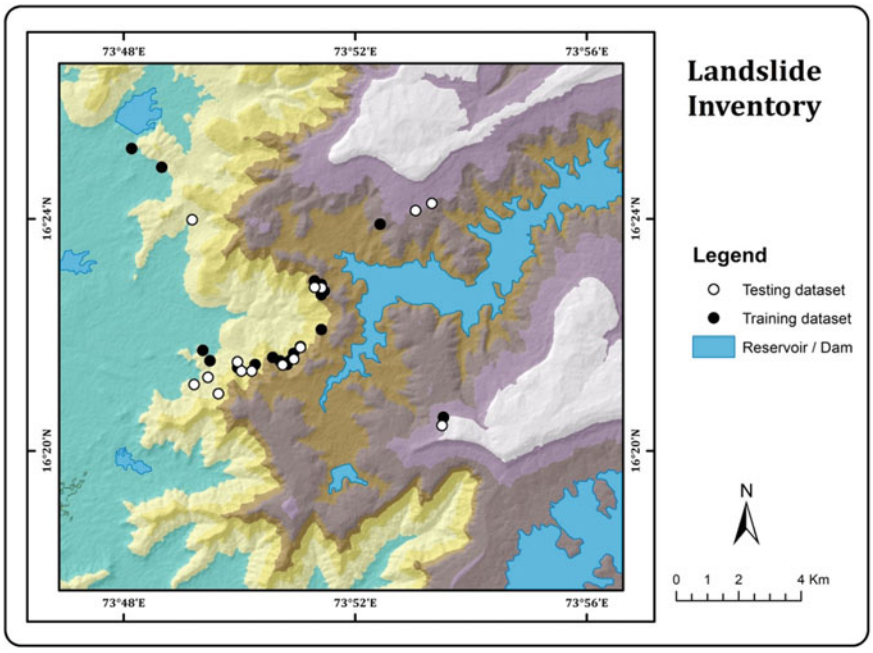

Fig. 2.3 Landslide inventory

identified 34 landslide point locations in the study area (Fig. 2.3). In which, 20 landslides are used as a training dataset for FR model while 14 are utilized for the model testing or assessment. The landslide inventory of the study area shows that most of the landslides have occurred along the road.

2.4.2 Influential Geo-environmental Factors of Landslide

2.4.2.1 Geology

Geology or rock type is an important factor in controlling slope stability. It controls the nature of the weathering and erosion of the region (Citrabhuwana et al. 2016). The Western Ghats is the vital orographic feature of Peninsular India, which denotes the long-lived uplift history. It is rugged, faulted, and eroded edge of the Deccan Plateau (Envi. & Forest Gov of India 2013). The spatial distribution of different rock types of the study area with geological formation is shown in Fig. 2.4. It has been observed that nine geological features existed in the study area viz. Deccan trap, Essentially Aa simple flow, Granite, Laterite, Mainly Aasimple flow, Megacryst flow, Quartz chlorite amphibole schist, Quartzite (Sedimentary) and Shale.

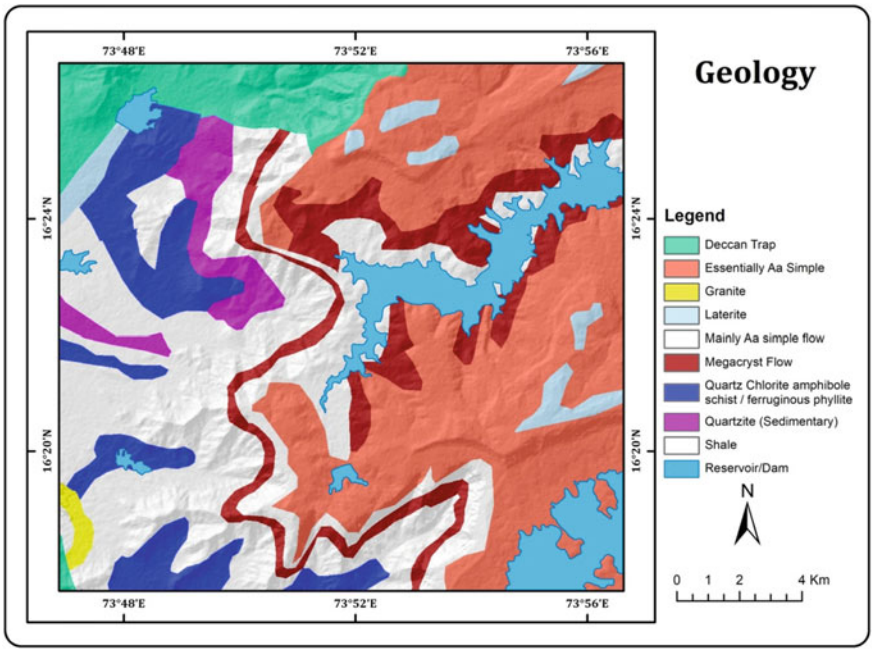

Fig. 2.4 Geology

2.4.2.2 Geomorphology

Geomorphology is science that studies the origin, evolution, and development of topographic features and how those topographies associate to form landscapes (Stetler 2014). The South Indian tectonic shield landscape is believed to have formed through a slow geomorphic process (Radhakrishna 1993). The spatial distribution of different landforms of the study area (Geomorphic Units) is shown in Fig. 2.5. It is being observed that six geomorphic landforms existed in the study area viz. Anthropogenic Origin-Anthropogenic Terrain, Denudational Origin-Mod Dissected Upper Plateau, Denudational Origin-Pediment-PediPlain Complex, Structural Origin-Low Dissected Lower Plateau, Structural Origin-Moderately Dissected Lower Plateau and Waterbody.

2.4.2.3 Drainage

In Peninsular India, Western Ghats is the major water divider for the east and west-flowing rivers. The rivers originate in the Western Ghats, flow down the steep scarp on the west and meet to the Arabian Sea, or they flow east, on the gently sloping plateaus and drain into the Bay of Bengal. The study area includes large numbers of small gullies, small streams, and tributaries (Fig. 2.6). The landslide analysis has

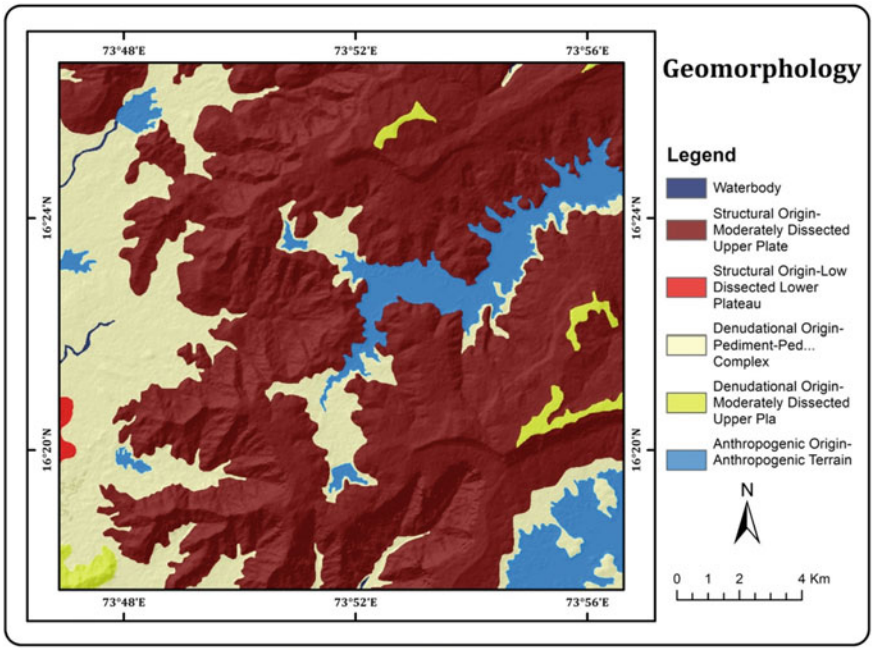

Fig. 2.5 Geomorphology

been done by using drainage distance. The drainage distance has been categorized into five categories in the study area viz. less than 200, 500, 1000, 2000 m, and more than 10000 m.

2.4.2.4 Relief

The relief of the Western Ghats of Maharashtra has two major parts that are Konkan and Ghat (Desh) region. Both regions reveal greater differences in elevation. The relief differs remarkably from place to place and the wide relief changes are seen in the west–east direction of Western Ghats with local variations (Deshpande 1971). The part of Konkan of the study area shows the greatest changes in elevation, whereas the plateau (Ghati) part is quite a monotonous feature with the least elevation change (Fig. 2.7). The relief is categorized into seven categories in the study area viz. less than 110 m, 111–241 m, 242–416 m, 417–565 m, 566–664 m, 665–785 m, and 786–948 m. The maximum height is 948 m, which is observed along the ridgeline of the Western Ghats in the study area. The lowest point is towards the extreme west part, where the height is 105 m above sea level. Comparatively, the western part of the study area has a lower elevation, whereas the eastern part of the study area is covered by higher elevation.

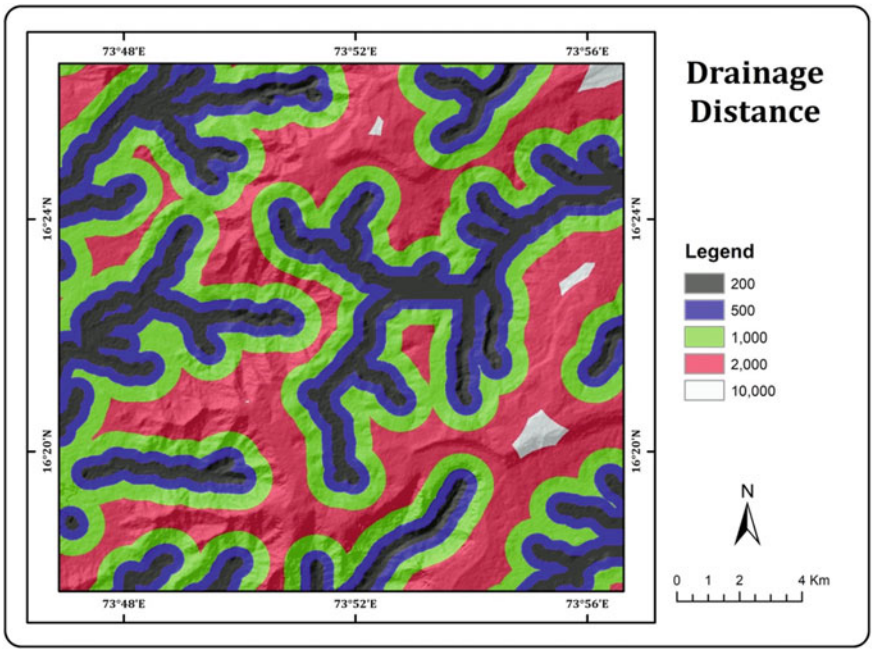

Fig. 2.6 Drainage distance

2.4.2.5 Slope

The geometry of slope is an important factor that affects slope stability (Chaulya et al. 2016). The degree or angle of slope very much governs the movement and extent of the landslide (Donnarumma et al. 2013; Chen et al. 2016). The slope map of the study area is prepared by using ALOS Pulsar DEM, which has 12.5 m spatial resolution. The slope of the entire study area has been divided into five categories, from 0 to 78 degrees range (Fig. 2.8). The ridgeline of the mountain range of Western Ghats is located at the center of the study area, which shows a greater degree of slope.

2.4.2.6 Land Use/Land Cover

Land Use and Land Cover (LU/LC) replicates the physical and socio-economical characteristics of land or surface of the earth (Mohammed et al. 2014). According to Rajan K.S and Shibasaki R (2001), Land Use and Land Cover is a significant component in understanding the interactions of human activities with the environment. The LU/LC map of the study area is prepared with a depiction of LU/LC unit viz. Barren Rocky, Deciduous Forest, Evergreen / Semi-evergreen, Fallow, Plantation, River, Rural, Scrub Forest, and Water Bodies/Reservoir (Fig. 2.9).

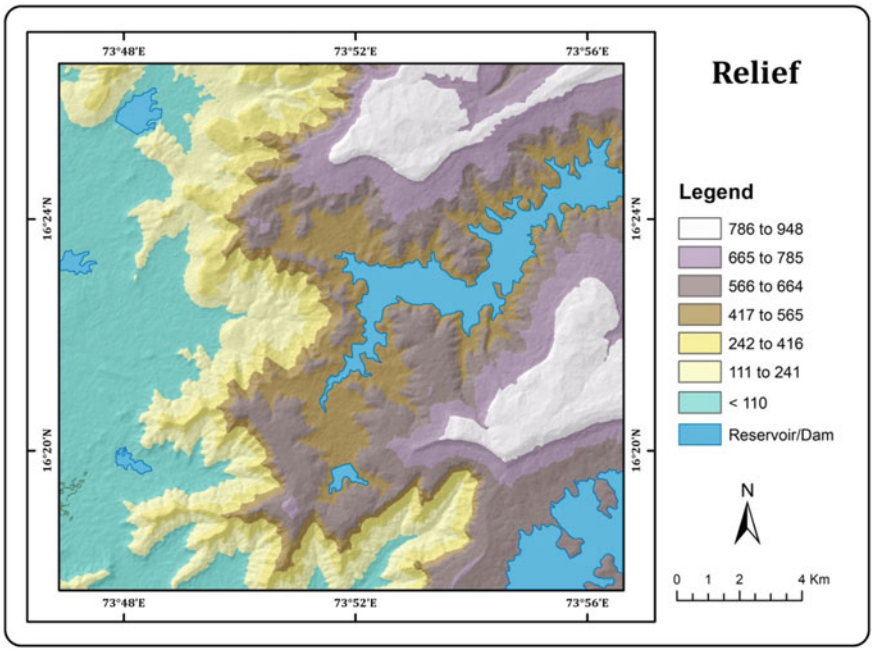

Fig. 2.7 Relief

2.4.2.7 Lineament

The lineaments are significant lines of the landscape caused by joints and faults, revealing the hidden architecture of the rock basement (Hobbs 1904). The structural geology of the area has a significant influence on the occurrence of landslides (Anbalagan and Singh 1996; Atkinson et al. 1998). Occurrences of landslides are mostly acknowledged in the areas of linear patterns or lineaments (Nagarajan et al. 1998a, 1998b). The lineaments are detected and mapped in the study area by using remote sensing data and GIS techniques. The Lineament Distance has been used as a landslide influencing factor, which is categorized into seven categories viz. 500, 1000, 3000 and 5000 m. While analyzing the lineament map, it is observed that about 39 lineaments have been passing through the area under investigation (Fig. 2.10).

2.4.2.8 Rainfall

Rainfall is recognized as a main triggering factor to create slope instability and further causing the occurrence of a landslide (Chen et al. 2003; Seul Bi Kim et al. 2015; OgbonnayaIgwe 2015; Aristizábal et al. 2017). In the study area, the western slopes of the mountains experience heavy rainfall (during the southwest monsoon from June to September), while the eastern slopes have moderate rainfall. The great

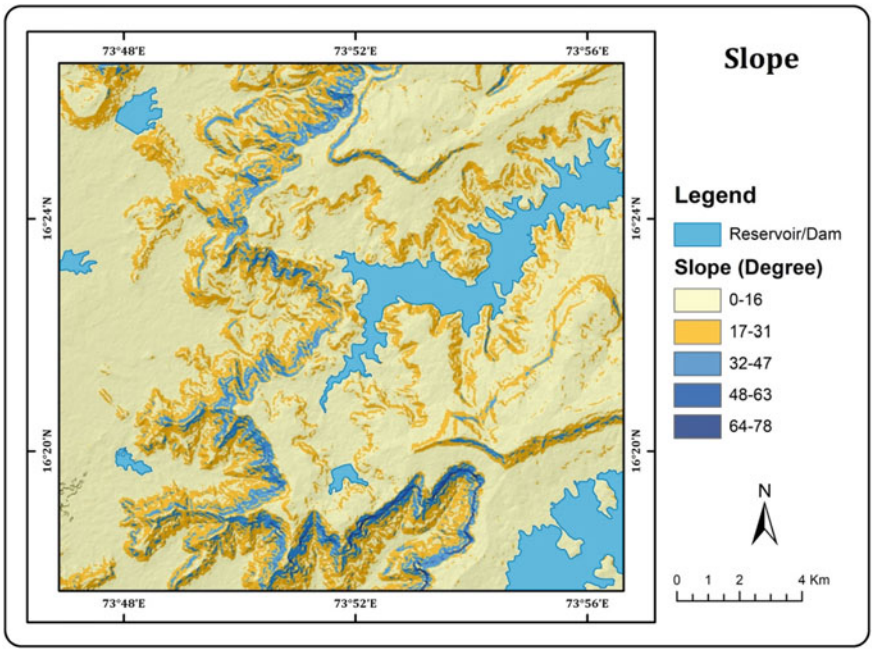

Fig. 2.8 Slope

variation of rainfall patterns in the Western Ghats also produces a great variety of vegetation types (Envi. & Forest Gov of India 2013). The distribution of rainfall in the study area is divided into four categories viz. 3001–3200 mm, 3201–3400 mm, 3401–3600 mm, and 3601–3800 mm. The annual average rainfall in this part is 3400 mm. The isohyet of rainfall of the study area reveals that the rainfall increases from east to west (Fig. 2.11).

2.4.2.9 NDVI

The dense vegetation cover reduces the impact of weathering and erosion, which increases slope stability, whereas the lands without vegetation cover are usually enhancing weathering and erosion of the slope. Thus it is responsible for slope failure (Normaniza et al. 2011; Normaniza et al. 2018). The wide variation of rainfall patterns in the Western Ghats also produces a great variety of vegetation types (Envi. & Forest Gov of India 2013). Ultimately, Normalized Difference Vegetation Index (NDVI) is an essential parameter to detect the concentration of vegetation for landslide studies. In the present research, the NDVI map is prepared by using Sentinel 2 satellite images (Fig. 2.12).

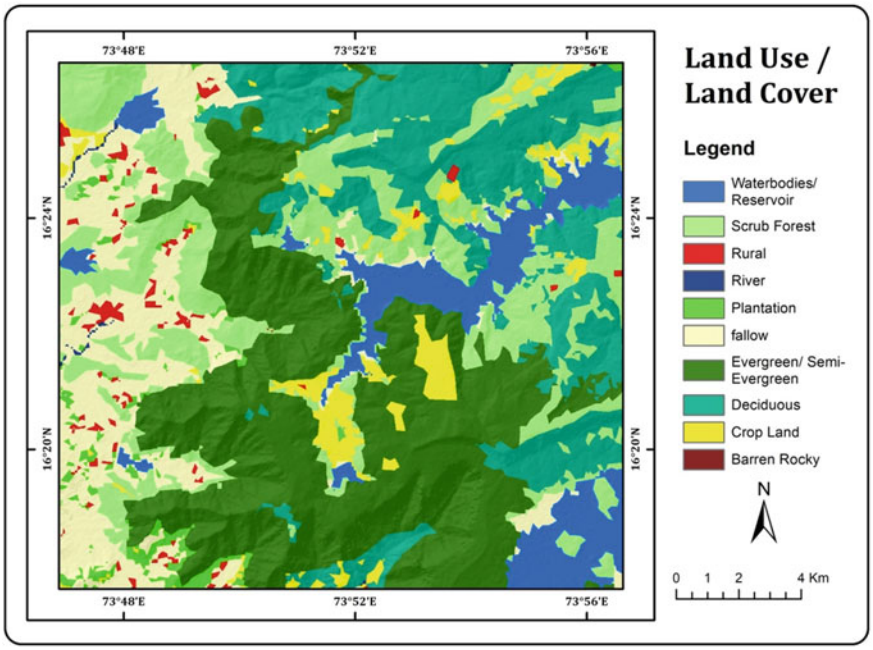

Fig. 2.9 Land use/land cover

Aspect

Aspect is one of the important topographic factors which affects a landslide (Hossein et al. 2014). The orientation of slope affects the distribution of sunlight, wind, and rainfall, thus indirectly affect to landslide occurrence (Clerici et al. 2006). The aspect map of the study area (Fig. 2.13) was produced by using the aspect tool of ArcGIS Software. The aspect of the study area is categorized into flat, north, northeast, east, southeast, south, southwest, west, and northwest facing classes from 0 to 360°.

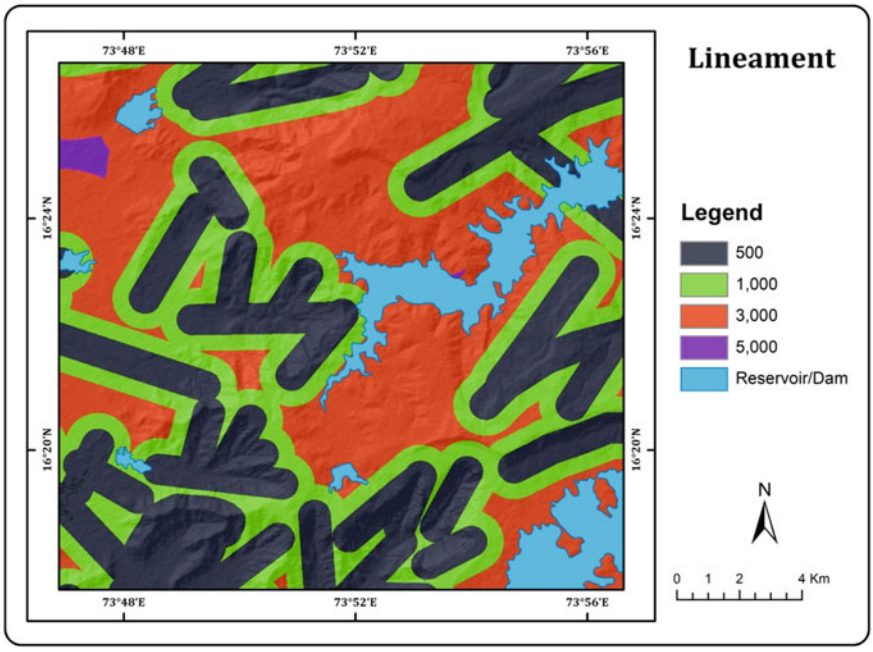

Fig. 2.10 Lineament

Curvature

Profile and plan curvatures of the slope are used for landslide investigation (Ayalew and Yamagishi 2004). Both profile and plan curvatures of a slope affect the landslide susceptibility (Carson and Kirkby 1972). The plan curvature of the slope is calculated using ALOS Pulsar DEM for the landslide susceptibility of the study area. The curvature map is classified into seven categories, from −33.91 to 33.27 value (Fig. 2.14).

Soil Depth

Soil depth is a crucial influential factor in slope stability and hillslope hydrology (Tromp-van Meerveld and McDonnell 2006). Soil depth factor is prepared by using a district resource map of the Geological Survey of India. The spatial distribution of soil depth of the study area is shown in Fig. 2.15. There are three classes of soli depth viz. Deep (>50 cm), Shallow (25–50 cm) and Very shallow (10–25 cm).

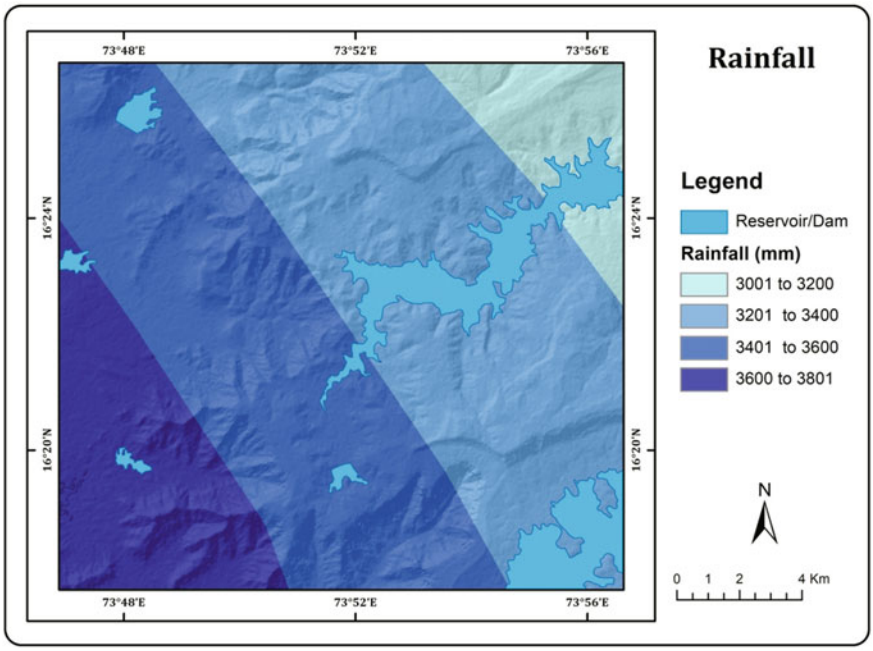

Fig. 2.11 Rainfall

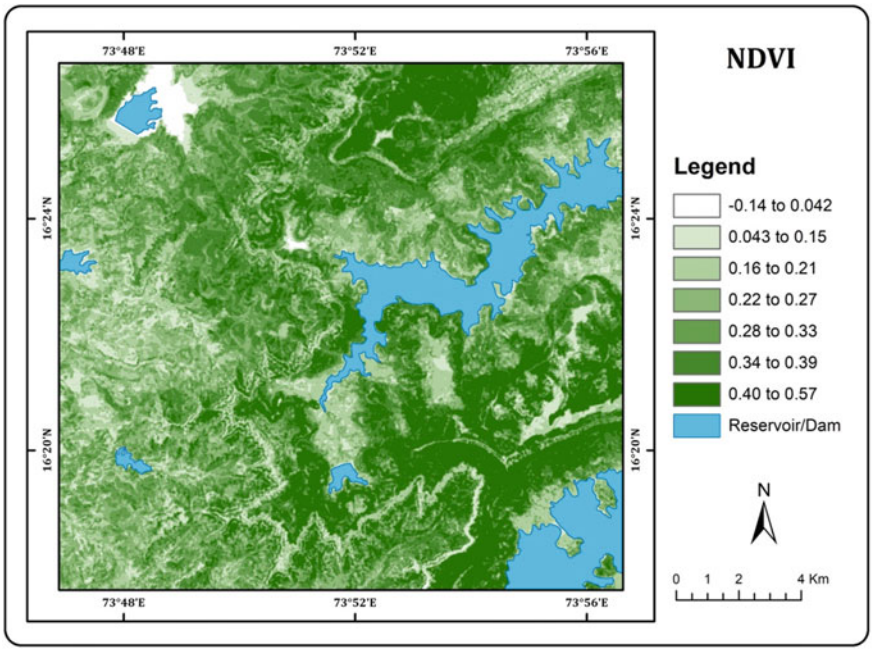

Fig. 2.12 Normalized difference vegetation index

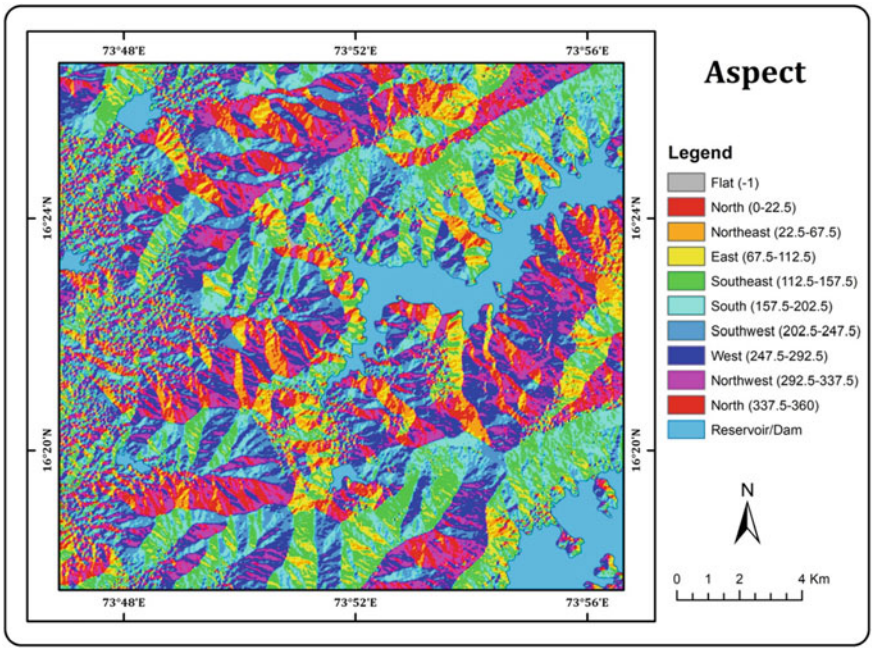

Fig. 2.13 Aspect

2.4.3 LSA by Frequency Ratio

For the present landslide investigation, the frequency ratio is calculated, which reveals the spatial relationships among the landslides inventory and influential factors (Table 2.1). The LSI values of PhondaGhat area range from 1.11 to 11.98. A higher LSI suggests a higher vulnerability to landslide occurrence. This study implements the equal interval method to classify the calculated LSI values into five categories: very high (1.39%), high (12.18%), moderate (35.49%), low (42.79%), and very low landslide susceptibility (8.16%) for easy and visual interpretation (Table 2.2). The susceptibility map (Fig. 2.16) demonstrates that about 13% of the land area of the study

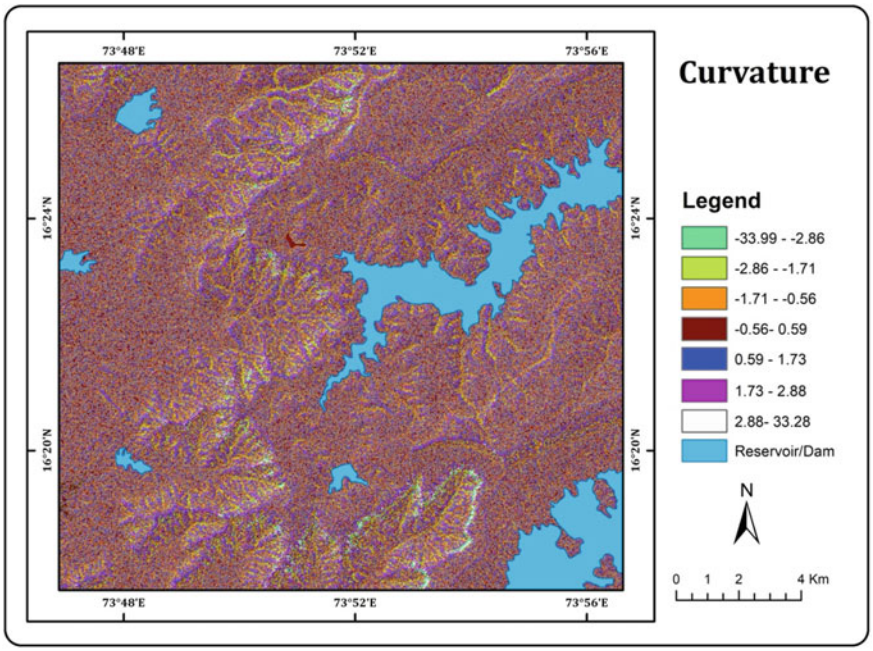

Fig. 2.14 Slope curvature

region is shown in the very high and high zone of landslide susceptibility. Hereafter, it is observed that most of the landslide-prone areas are found along State Highway No. 179.

2.4.4 Validation of the Frequency Ratio Model

In this study, a frequency ratio approach for estimating the susceptible areas of landslide using a GIS is applied and tested. Field investigation-based landslide inventory (Testing data) is used for the model validation. Area Under Curvature (AUC) is calculated from the cumulative percentage of susceptible zones of LSI in the study area and the cumulative percentage of landslide occurrences in the classes as per Table 2.3. As per the result, the AUC value of 0.823 is obtained for the frequency ratio. It shows the accuracy of the model (Fig. 2.17). The intensive field investigation is carried out in the study area for validation of the result (Fig. 2.18).

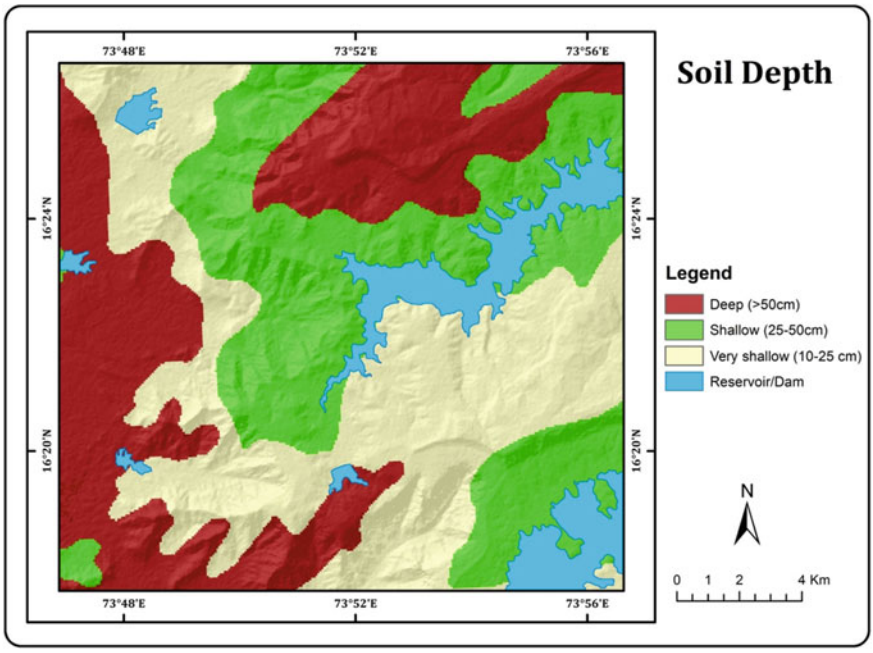

Fig. 2.15 Soil depth

2.5 Conclusion

The present study illustrates that the landslide susceptibility mapping of Phonda Ghats of Maharashtra. The Frequency Ratio model is applied and tested using Remote Sensing and GIS techniques. The susceptibility map shows that more than 13% of the land area of the study region is highly susceptible to the occurrence of the landslide. Hence, the major portion along PhondaGhatroad (SH-179) is represented as highly vulnerable to the landslide. Therefore, this road is dangerous for unplanned anthropogenic activities. The study reveals that the frequency ratio is an effective method for landslide susceptibility mapping of hilly and rugged mountainous areas. The performance of the Frequency Ratio model is validated by cumulative frequency diagram, which shows that the model has an accuracy of 82% based on field investigation. The landslide susceptibility map will be useful for planners and engineers in choosing locations for the prevention and mitigation of existing and future landslides.

Table 2.1 Result of FR model for each factor

Factors	Class	No. of landslide	Landslide (%)	No of pixel in domain	Area (%)	Frequency ratio	Normalization
Drainage	200	1	5	206,334	16	0.31	0.15
	500	1	5	276,820	21	0.23	0.11
	1000	5	25	407,165	31	0.79	0.37
	2000	13	65	391,131	30	2.15	1
	10,000	0	0	12,415	1	0	0
Geology	Deccan Trap	0	0	93,356	7	0	0
	Laterite	0	0	36,313	3	0	0
	Megacryst Flow	4	20	138,942	11	1.86	0.87
	Mainly a simple flow	13	65	393,404	30	2.14	1.00
	Essentially a simple flow	1	5	438,908	34	0.15	0.07
	Quartzite (Sedimentary)	0	0	43,645	3	0.00	0
	Shale	0	0	29,181	2	0.00	0
	Quartz Chlorite amphibole schist/ferruginous phyllite	2	10	113,504	9	1.14	0.53
	Granite	0	0	6,612	1	0	0
Geomorphology	Structural origin-moderately dissected upper plateau	19	95	874,983	68	1.40	1
	Denudational origin-moderately dissected upper plateau	0	0	21,125	2	0.00	0

(continued)

Table 2.1 (continued)

Factors	Class	No. of landslide	Landslide (%)	No of pixel in domain	Area (%)	Frequency ratio	Normalization
	Denudational origin-pediment-pediplain complex	1	5	282,778	22	0.23	0.16
	Anthropogenic origin-anthropogenic terrain	0	0	109,740	8	0	0
	Waterbody	0	0	2,301	0	0	0
	Structural origin-low dissected lower plateau	0	0	2,938	0	0	0
Lineament	500	7	35	459,827	36	0.98	0.73
	1000	7	35	337,709	26	1.34	1.00
	3000	6	30	484,439	37	0.80	0.60
	5000	0	0	11,890	1	0	0
LULC	Rural	0	0	14,785	1	0	0
	Crop land	0	0	57,245	4	0	0
	Plantation	0	0	22,153	2	0	0
	Fallow	2	10	173,499	13	0.75	0.32
	Evergreen/Semi-evergreen	15	75	414,769	32	2.34	1
	Deciduous	1	5	248,214	19	0.26	0.11
	Scrub forest	2	10	251,671	19	0.51	0.22
	Barren rocky	0	0	97	0	0	0
	River	0	0	1,525	0	0	0
	Waterbodies/Reservoir	0	0	109,907	8	0	0

(continued)

Table 2.1 (continued)

Factors	Class	No. of landslide	Landslide (%)	No of pixel in domain	Area (%)	Frequency ratio	Normalization
NDVI	– 0.14 to 0.042	0	0	67,698	5	0	0
	0.043–0.15	0	0	94,464	7	0	0
	0.16–0.21	4	20	179,804	14	1.44	0.94
	0.22–0.27	4	20	229,535	18	1.13	0.73
	0.28–0.33	6	30	252,323	20	1.54	1
	0.34–0.39	5	25	244,662	19	1.32	0.86
	0.40–0.57	1	5	225,379	17	0.29	0.19
Rainfall	3201–3400	4	20	540,558	42	0.48	0.21
	3600–3801	0	0	200,848	16	0	0
	3401–3600	16	80	451,239	35	2.29	1
	3001–3200	0	0	101,220	8	0	0
Elevation	<110	2	10	267,210	21	0.48	0.10
	111–241	2	10	165,391	13	0.78	0.15
	242–416	9	45	114,646	9	5.08	1
	417–565	5	25	254,266	20	1.27	0.25
	566–664	1	5	259,186	20	0.25	0.05
	665–785	1	5	194,923	15	0.33	0.07
	786–948	0	0	38,243	3	0	0
Slope	0–16	4	20	919,223	71.04	0.28	0.10
	17–31	13	65	297,697	23.01	2.83	1
	32–47	3	15	70,323	5.44	2.76	0.98

(continued)

Table 2.1 (continued)

Factors	Class	No. of landslide	Landslide (%)	No of pixel in domain	Area (%)	Frequency ratio	Normalization
	48–63	0	0	5,671	0.44	0	0
	64–78	0	0	951	0.07	0	0
Slope curvature	−33.91999817 to − 2.855695834	0	0	8,517	0.7	0	0
	−2.855695833 to − 1.707654161	3	15	62,724	4.8	3.09	0.42
	−1.70765416 to − 0.559612488	4	20	399,969	30.9	0.65	0.09
	− 0.559612488 to 0.588429185	3	15	354,344	27.4	0.55	0.07
	0.588429185–1.736470858	8	40	397,075	30.7	1.30	0.18
	1.736470859–2.884512532	1	5	62,530	4.8	1.03	0.14
	2.884512533–33.27999878	1	5	8,706	0.7	7.43	1.00
Soil	Deep & moderately deep (depth > 50 cm)	0	0	375,944	29.06	0	0
	Shallow (25–50 cm)	15	75	453,928	35.08	2.14	1
	Very shallow (10–25 cm)	5	25	463,993	35.86	0.70	0.33
Aspect	0.5162–45.45	3	15	129,954	10.0	1.49	0.63
	45.46–90.39	2	10	103,952	8.0	1.24	0.53
	90.4–135.3	1	5	147,952	11.4	0.44	0.19

(continued)

Table 2.1 (continued)

Factors	Class	No. of landslide	Landslide (%)	No of pixel in domain	Area (%)	Frequency ratio	Normalization
	135.4–180.3	0	0	199,217	15.4	0	0
	180.4–225.2	3	15	179,886	13.9	1.08	0.46
	225.3–270.1	3	15	172,906	13.4	1.12	0.48
	270.2–315.1	2	10	195,522	15.1	0.66	0.28
	315.2–360	6	30	164,476	12.7	2.36	1.00

Table 2.2 Landslide susceptibility zones

Sr. No	Susceptibility zone	No. of pixels within zone	Area of zone (%)
1	Very low	105,581	8.16
2	Low	553,620	42.79
3	Moderate	459,176	35.49
4	High	157,545	12.18
5	Very high	17,943	1.39

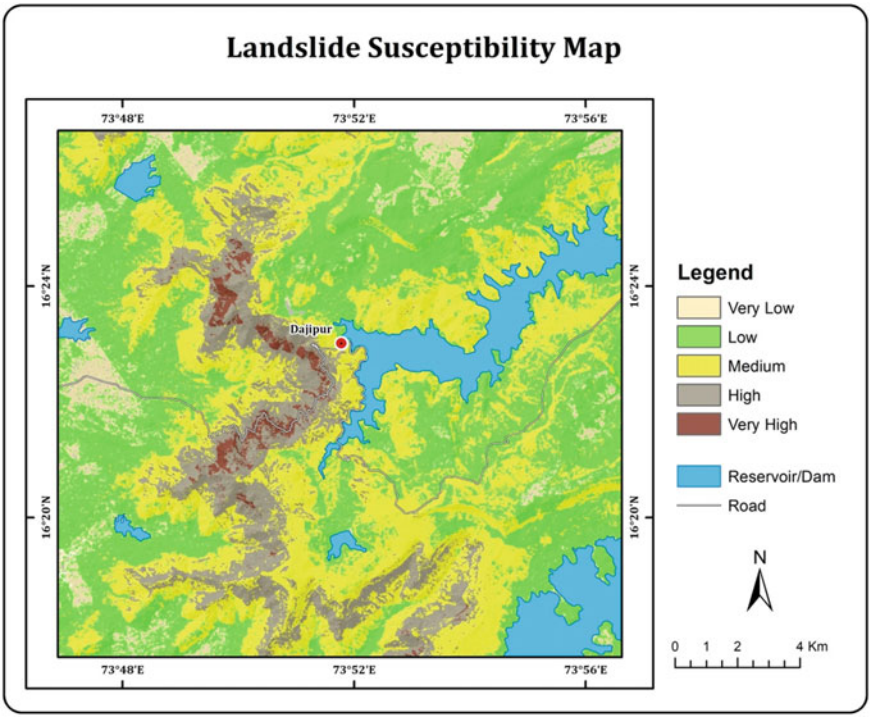

Fig. 2.16 Landslide susceptibility map using FR

Table 2.3 Distribution of susceptible classes and landslide occurrence

Susceptibility zone	No. of testing landslide	Percentage of testing landslide	Area percentage
Very low	0	0	8.16
Low	1	6.67	42.79
Medium	4	26.67	35.49
High	6	40	12.18
Very high	4	26.67	1.39

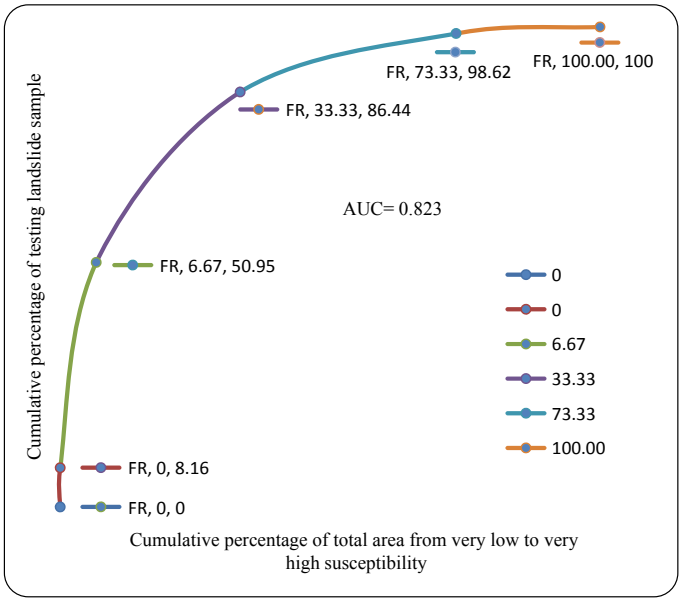

Fig. 2.17 Cumulative frequency diagram showing landslide susceptibility classification in the cumulative percentage of landslide occurrence

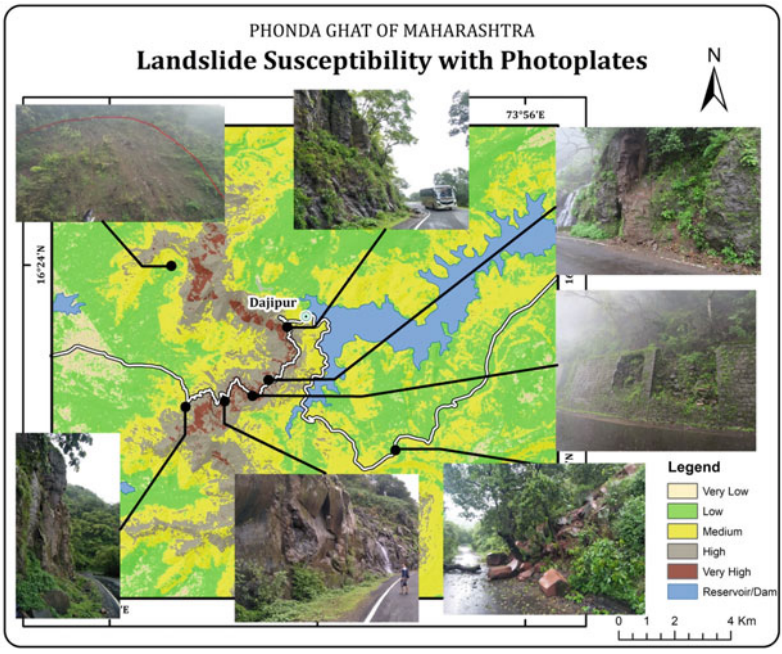

Fig. 2.18 Photo-plates of field investigation

References

Ahmed B (2014) Landslide Susceptibility mapping using multi-criteria evaluation techniques in Chittagong Metropolitan Area Bangladesh. Landslides 12:1077–1095. https://doi.org/10.1007/s10346-014-0521-x

Anbalagan R, Singh B (1996) Landslide hazard and risk assessment mapping of mountainous terrains- a case study from Kumaun Himalaya, India. EngGeol 43:237–246. https://doi.org/10.1016/S0013-7952(96)00033-6

Aristizábal E, Martínez-Carvajal H, García-Aristizábal E (2017) Modelling shallow landslides triggered by rainfall in tropical and mountainous basins. In: Mikoš M, Casagli N, Yin Y, Sassa K (eds) Advancing culture of living with landslides. WLF 2017. Springer, Cham. https://doi.org/10.1007/978-3-319-53485-5_23

Atkinson PM, Massari R (1998) Generalised linear modelling of susceptibility to landsliding in the Central Apennines. Italy. Comput Geosci 24(4):373–385. https://doi.org/10.1016/S0098-3004(97)00117-9

Ayalew L, Yamagishi H (2004) Slope failures in the Blue Nile basin, as seen from landscape evolution perspective. Geomorphology 57:95–116. https://doi.org/10.1016/S0169-555X(03)00085-0

Balasubramani K, Kumaraswamy K (2013) Application of geospatial technology and Information value technique in landslide hazard zonation mapping: a case study of Giri valley Himachal Pradesh. Disaster Adv 6(1):38–47

Bello MN, Abbas II and Akpu B (2014) Analysis of land use-land cover changes in Zuru and its environment of Kebbi state, Nigeria using remote sensing and geographic information system technology. J Geogr Earth Sci 2:113–126

Carson MA, Kirkby MJ (1972) Hillslope form and process. Cambridge University Press, London, p 475

Chaulya, S. K., & Prasad, G. M. (2016) Slope Failure Mechanism and Monitoring Techniques. Sensing and Monitoring Technologies for Mines and Hazardous Areas, 1–86. https://doi.org/10.1016/B978-0-12-803194-0.00001-5

Chen H, Lee CF (2003) A dynamic model for rainfall-induced landslides on natural slopes. Geomorphology 51(4):269–288. https://doi.org/10.1016/S0169-555X(02)00224-6

Chen XL, Liu C-G, Chang Z-F, Zhou Q (2016) The relationship between the slope angle and the landslide size derived from limit equilibrium simulations. Geomorphology 253:547–550. https://doi.org/10.1016/j.geomorph.2015.01.036

Citrabhuwana BN, Kusumayudha SB, Purwanto (2016) Geology and slope stability analysis using markland method on road segment of Piyungan–Patuk, Sleman and Gunungkidul regencies, Yogyakarta special region Indonesia. Int J Econ Environ Geol 7(1):42–52

Clerici A, Perego S, Tellini C, Vescovi P (2006) A GIS-based automated procedure for landslide susceptibility mapping by the Conditional Analysis method: the Baganza valley case study (Italian Northern Apennines). Environ Geol 50:941–961. https://doi.org/10.1007/s00254-006-0264-7

Deshpande CD (1971) Geography of Maharashtra, National book trust, India A-5 Green Park, New Delhi-16

Donnarumma A, Revellino P, Grelle G, Guadagno FM (2013) Slope angle as indicator parameter of landslide susceptibility in a geologically complex area. Landslide Sci Pract, 425–433. https://doi.org/10.1007/978-3-642-31325-7_56

Gupta RP, Saha AK, Arora MK and Kumar A (1999) Landslide hazard zonation in a part of the Bhagirathi valley, Garhwal Himalayas, using integrated remote sensing—GIS. Himal Geol 20:71–85

Gupta R, Joshi B (1990) Landslide hazard zoning using the gis approach—a case study from the Ramganga catchment, Himalayas. Eng Geol 28:119–131. https://doi.org/10.1016/0013-7952(90)90037-2

Guzzetti F, Carrara A, Cardinali M, Reichenbach P (1999) Landslide hazard evaluation: a review of current techniques and their application in a multi-scale study. Central Italy, Geomorphology 31:181–216

Hobbs WH (1904) Lineaments of the Atlantic border region. Geol Soc Am Bull 15:483–506

Igwe O (2015) The study of the factors controlling rainfall-induced landslides at a failure-prone catchment area in Enugu, Southeastern Nigeria using remote sensing data. Landslides 12:1023–1033. https://doi.org/10.1007/s10346-015-0627-9

Kayastha P, Dhital MR and De Smedt F (2013) Application of the analytical hierarchy process (AHP) for landslide susceptibility mapping: a case study from the Tinau watershed, West Nepal. Comput Geosci 52:398–408. https://doi.org/10.1016/j.cageo.2012.11.003

Kim SB, Na JH and Seo YS (2015) Prediction of rainfall-induced slope failure using Hotelling's T-Square statistic. J Eng Geol 25(3):331. https://doi.org/10.9720/kseg.2015.3.331

Lee S, Min K (2001) Statistical analysis of landslide susceptibility at Yongin, Korea. Environ Geol 40:1095–1113

Lee S and Pradhan B (2006) Probabilistic landslide hazards and risk mapping on Penang Island, Malaysia. J Earth Syst Sci 115(6):661–672. https://doi.org/10.1007/s12040-006-0004-0

Lee S, Choi J and Min K (2004) Probabilistic landslide hazard mapping using GIS and remote sensing data at Boun, Korea. Int J Remote Sens 25(11):2037–2052. https://doi.org/10.1080/01431160310001618734

Lee S, Oh H, Park NW (2007) Extraction of landslide-related factors from ASTER imagery and its application to landslide susceptibility mapping using GIS. IEEE international geoscience and remote sensing symposium, Barcelona, Spain

Lee S, Talib JA (2005) Probabilistic landslide susceptibility and factor effect analysis. Environ Geol 47:982–990. https://doi.org/10.1007/s00254-005-1228-z

Mahalingam R, Olsen MJ, O'Banion MS (2016) Evaluation of landslide susceptibility mapping techniques using lidar-derived conditioning factors (Oregon case study). Geomat Nat Hazards Risk. 7(6):1–24. https://doi.org/10.1080/19475705.2016.1172520

Mantovani F, Soeters R, Van Westen CJ (1996) Remote sensing techniques for landslide studies and hazard zonation in Europe. Geomorphology 15(3–4):213–225. https://doi.org/10.1016/0169-555X(95)00071-C

Masoumi H, Jamali AA, Khabazi M (2014) Investigation of role of slope, aspect and geological formations of landslide occurrence using statistical methods and GIS in some watersheds in ChaharMahal and Bakhtiari province. J Appl Environ Biol Sci 4(9):121–129

Merrett HC, Chen WW (2013) Applications of geographical information systems and remote sensing in natural disaster hazard assessment and mitigation in Taiwan. Geomat Nat Haz Risk 4(2):145–163. https://doi.org/10.1080/19475705.2012.686064

Ministry of Environment and Forests Government of India (2013) Report of the high level working group on Western Ghats, vol 1. http://www.uttarakannada.nic.in/docs/Publication/HLWGWESTERNGHATSVOLUME1.pdf

Nagarajan R, Mukherjee A, Roy A, Khire MV (1998a) Temporal remote sensing data and GIS application in landslide hazard zonation of part of Western Ghat, India. Int J Remote Sens 19:573–585

Nagarajan R, Mukherjee A, Roy A and Khire MV (1998b) Technical note temporal remote sensing data and GIS application in landslide hazard zonation of part of Western ghat, India. Int J Remote Sens 19(4):573–585

Normaniza O, Barakbah SS (2011) The effect of plant succession on slope stability. Ecol Eng 37:139–147. https://doi.org/10.1016/j.ecoleng.2010.08.002

Normaniza O, Aimee H, Ismail 0y, Tan G Y A and Rozainah M Z (2018) Promoter effect of microbes in slope eco-engineering: effects on plant growth, soil quality and erosion rate at different vegetation densities. Appl Ecol Environ Res 16(3):2219–2232. https://doi.org/10.15666/aeer/1603_22192232

Pardeshi SD, Autade SE, Pardeshi SS (2013) Landslide hazard assessment: recent trends and techniques. Springerplus 2013(2):523. https://doi.org/10.1186/2193-1801-2-523

Patil AS, Bhadra BK, Panhalkar SS, Patil PT (2020) Landslide susceptibility mapping using landslide numerical risk factor model and landslide inventory prepared through OBIA in Chenab Valley, Jammu and Kashmir (India). J Indian Soc Remote Sens 48:431–449. https://doi.org/10.1007/s12524-019-01092-5

Patil AS, Panhalkar S (2019) Analytical hierarchy process for landslide hazard zonation of South-Western ghats of Maharashtra, India. Disaster Adv 12:26–39.

Persichillo MG, Bordoni M, Meisina C, Bartelletti C, Barsanti M, Giannecchini R, Avanzi GDA, Galanti Y, Cevasco A, Brandolini P (2016) Shallow landslides susceptibility assessment in different environments. Geom Nat Hazards Risk 8(2):748–771. https://doi.org/10.1080/19475705.2016.1265011

Pradhan B, Lee S (2010) Landslide susceptibility assessment and factor effect analysis: backpropagation artificial neural networks and their comparison with frequency ratio and bivariate logistic regression modelling. Environ Modell Softw 25(6):747–759. https://doi.org/10.1016/j.envsoft.2009.10.016

Qiao G et al (2013) Landslide investigation with remote sensing and sensor network: from susceptibility mapping and scaled-down simulation towards in situ sensor network design. Remote Sens 5:4319–4346. https://doi.org/10.3390/rs5094319

Radhakrishna BP (1993) Neogene uplift and geomorphic rejuvenation of the Indian Peninsula. Curr Sci 64(11&12):787–793

Rajan K and Shibasaki R (2001) A GIS-based integrated land use/cover change model to study agricultural and urban land-use changes. In: Proceedings of 22nd Asian conference on remote sensing. https://crisp.nus.edu.sg/~acrs2001/pdf/250Rajan.pdf

Ramachandra TV, Kumar U, Aithal B (2010) Landslide Susceptible Locations in Western Ghats: Prediction through OpenModeller

Saha AK, Gupta RP, Arora MK (2002) GIS-based landslide hazard zonation in the Bhagirathi (Ganga) Valley. Himalayas. Int J Remote Sens 23(2):357–369. https://doi.org/10.1080/01431160010014260

Scaioni M (2013) Remote sensing for landslide investigations: From research into practice. Remote Sens 5:5488–5492. https://doi.org/10.3390/rs5115488

Srivastava V, Srivastava HB, Lakhera RC (2010) Fuzzy gamma based geomatic modelling for landslide hazard susceptibility in a part of tons river valley, northwest Himalaya. India. Geom Nat Hazards Risk. 1(3):225–242. https://doi.org/10.1080/19475705.2010.490103

Stetler LD (2014) Geomorphology. Ref Modul Earth Syst Environ Sci. https://doi.org/10.1016/B978-0-12-409548-9.09078-3

Tromp-van Meerveld, H.J., McDonnell, J.J (2006) Threshold relations in subsurface stormflow: 2. The fill and spill hypothesis. Water Resour Res, W02411. https://doi.org/10.1029/2004WR003800

Varnes DJ (1984) Landslide hazard zonation: a review of principles and practices commission on landslides of the IAEG. UNESCO, Paris

van Wstern CJ, Ghosh S, Jaiswal P, Martha TR and Kuriakose SL (2011): From landslide inventories to landslide risk assessment; an attempt to support methodological development in India, the second world landslide forum. Rome, pp 3–7

Wang Q, Li W, Yan S, Wu Y, Pei Y (2016) GIS based frequency ratio and index of entropy models to landslide susceptibility mapping (Daguan, China). Environ Earth Sci 75(9):1–16. https://doi.org/10.1007/s12665-016-5580-y

Wang HB, Sassa K (2005) Comparative evaluation of landslide susceptibility in Minamata area, Japan. Environ Geol 47:956–966. https://doi.org/10.1007/s00254-005-1225-2

Westen et al., 1999.Van Westen CJ, Seijmonsbergen AC, Mantovani F (1999) Comparing landslide hazard maps. Nat Hazards 20:137–158

Yilmaz I (2009) Landslide susceptibility mapping using frequency ratio, logistic regression, artificial neural networks and their comparison: a case study from Kat landslides (Tokat–Turkey). Comput Geosci 35:1125–1138. https://doi.org/10.1016/j.cageo.2008.08.007